A R C H I V E S O F M E T A L L U R G Y A N D M A T E R I A L S
Volume 50 2005 Issue 3

E. HADASIK*

METHODOLOGY FOR DETERMINATION OF THE TECHNOLOGICAL PLASTICITY CHARACTERISTICS BY HOT TORSION TEST

METODYKA WYZNACZANIA CHARAKTERYSTYK TECHNOLOGICZNEJ PLASTYCZNOŚCI W PRÓBIE SKRĘCANIA NA GORĄCO

A procedure for determination of the relationship between flow stress and strain by hot torsion test is presented in the paper. This procedure takes into account preparation of samples for plastometric tests, heating of samples, elaboration of torsion test results and selection of the sample representative area for the microstructure examination. During elaboration of test results, the following operations are considered: processing of measurement signals (filtration, decimation, trimming and smoothing), correction of torque (due to twist rate and temperature discrepancies) and correction of strain (due to the non-uniformity of strain along the sample gauge length). Diversity of microstructure over the sample cross-section due to non-uniformity of strain is demonstrated. It proves the necessity of determining the sample representative area for comparative microstructure examinations.

W artykule podano procedurę wyznaczania zależności naprężenia uplastyczniającego od odkształcenia na podstawie prób skręcania na gorąco. Procedura ta uwzględnia przygotowanie próbek do badań plastometrycznych, nagrzewanie próbek, opracowanie wyników prób skręcania oraz sposób pobrania próbki do oceny mikrostruktury. Przy opracowaniu wyników badań uwzględniono obróbkę sygnałów pomiarowych polegającą na ich filtracji, przerzedzaniu oraz wygładzaniu, korektę momentu skręcającego ze względu na zróżnicowanie prędkości skręcania i temperatury oraz korektę odkształcenia ze względu na nierównomierny rozkład odkształceń na długości próbki. Wykazano zróżnicowanie mikrostruktury na przekroju próbki wynikające ze zróżnicowania odkształcenia oraz wskazano na konieczność określenia obszaru reprezentatywnego do porównawczej oceny mikrostruktury materiału.

1. Introduction

Both the data in literature as well as our own experience confirm a big practical application of plastometric torsion test. Such test is especially useful for determination

* DEPARTMENT OF PROCESS MODELLING AND MEDICAL ENGINEERING, 40-019 KATOWICE, KRASIŃSKIEGO 8, POLAND

of the material technological plasticity characteristics which represent the true properties of material in a metal forming process. It is used also for comparative evaluation of material plasticity depending on its chemical composition, phase composition and production technology [1-6].

The experience gained till now in the methodology of plastometric torsion test realization confirms that the quality and correctness of plastometric test results depend on such factors as [7]:

- advancement of design and capability of a torsion plastometer control system,
- method of sampling, preparation of the sample structure to correspond to the structure of material in a real production process,
- uniformity of sample heating and proper heating parameters,
- selection of a sample shape and a sample size,
- correctness of recording, processing and interpretation of signals,
- methodology of the flow stress determination, basing on theoretical formulas,
- considering the effect of sample temperature changes during deformation,
- considering the non-uniformity of strain over the gauge length and cross-section of a sample.

Diversity in the modernity level of torsion plastometers, flexibility in the method of testing, difficulties in considering the thermal effect and the non-uniformity of strain lead to significant discrepancies between results obtained in various research centres.

It can be stated that there does not exist one generally accepted method allowing for determination of the relation between flow stress σ_p and strain ε from recordings of torque M and number of twists N (torsion angle) obtained in the hot torsion test. A very high non-uniformity of strain and diversification of strain rate $\dot{\varepsilon}$ over the sample cross-section make it impossible to find any simple relations allowing for correct determination of a stress-strain curve in the hot torsion test. Modelling of the torsion test using the finite elements method [8] also requires application of many oversimplifications, and in the nearest future it would not find a general application.

2. Procedure for determination of technological plasticity characteristics

The experience gathered in scope of methodology and application of the plastometric torsion test had allowed for elaboration of the procedure aimed at standardization of test conditions. The methodology for test results processing had been developed, too. It allows for determination of technological plasticity characteristics with elimination of the interference effect from the non-uniformity of strain and from the instability of both thermal phenomena and twist rate. Such procedure, presented in Fig. 1, involves the following stages:

- preparation of samples for plastometric tests,
- heating of plastometric samples,
- performing the plastometric tests,
- defining the sample area for microstructure testing.

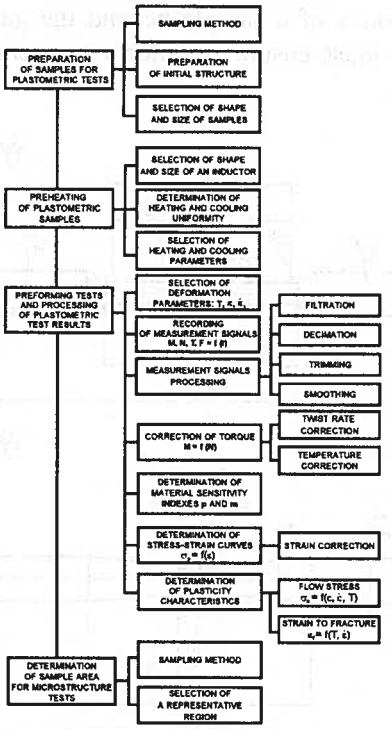

Fig. 1. Block flow diagram for determination of technological plasticity characteristics at the hot torsion test [7]

2.1. Preparation of samples for plastometric test

When taking samples from a tested element it should be considered that the method of sample preparation might have the essential effect on determined plasticity characteristics. This relates in particular to samples taken from an ingot, but also from a billet, sheet or flat. Direction of sampling should be clearly defined and it must consider the normal stress components orientation on account of directional properties of the microstructure.

The material structure of plastometric samples should correspond to the structure of a material deformed under industrial conditions. This refers in particular to alloy materials for which a long soaking time is required to obtain a proper material structure, corresponding to the structure of a material soaked under industrial conditions.

The sample geometry and accuracy of its preparation have essential influence on the test results [9]. The most stable conditions are being obtained for the sample diameter from 6 to 10 mm and the aspect ratio from $\frac{1}{3}$ to 10. These criteria are met by a sample having the diameter $D = 6$ mm and the gauge length $L = 50$ mm, therefore it should be generally used for torsion tests (Fig. 2a). When using higher strain rates, a sample of $D = 6$ mm and $L = 10$ mm can be used (Fig. 2b).

The shape and dimensions of a sample beyond the gauge length depend on the applied inductor and they must ensure a uniform temperature distribution over the gauge length.

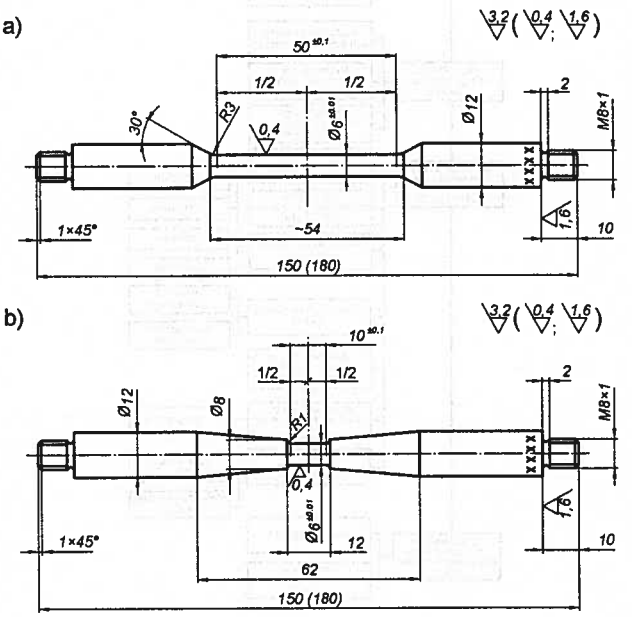

Fig. 2. Shape and dimensions of samples used for hot torsion tests: L = 50 mm (a), L = 10 mm (b) [7]

2.2. Heating of plastometric samples

Selection of heating parameters should consider the progress and structural effects of heating in the industrial metal forming processes, with subsequent cooling to a deformation temperature. This can prove to be impossible to be conducted in chamber furnaces. During heating in this furnace type, the excessive scale formation takes place on the sample surface due to long soaking times which are needed for temperature equalization. The time of heating and cooling, ensuring temperature equalization over the cross-section and the gauge length of a sample, depends on a heating method and physical properties of a tested material. For control of a temperature regime and a heating rate, the induction method is the most effective and should replace heating in chamber furnaces. A uniformity of heating can be ensured by appropriate design of an inductor [10].

2.3. Elaboration of plastometric test results

The quality of plastometric test results depends on: precision of the plastometer mechanical driving system and the plastometer control system, accuracy of the data

acquisition system and correctness of measurement signals recording, processing and interpretation. Measurements are affected by the discrepancies between assumed and actual test conditions and by the functioning of measuring circuits. Correctness of the test results depends on the capability of determining the causes of measurement disturbances, the capability of disturbances elimination during the measurement signals processing and the capability of determining the relations $M = f(N)$, $= f(N)$, $T = f(N)$ and $F = f(N)$. The common software packages such as "Matlab", "Excel" and "Octave" involve the effective tools for data processing. A prerequisite for correct processing of measurement signals and determination of the $M = f(N)$ relation is a good knowledge of mechanical and thermal phenomena accompanying the torsion process. Fulfilling this requirement in connection with the application of above mentioned software packages would allow for:

- graphic presentation of the raw measurement signals as well as the processed data after any data processing stage,
- performing the digital filtration of the measurement signals,
- processing of the filtered measurement signals,
- smoothing of the processed measurement signals,
- determination of the corrected relations $M = f(N)$,
- determination of the differential parameters p and m, necessary for defining the $\sigma_p = f(\varepsilon)$ relation.

Values of the flow stress defined at the torsion test depend on: considering the twist rate and temperature corrections in determination of the $M = f(N)$ relation, the method adopted for conversion of the torque curve $M = f(N)$ into the $\sigma_p = f(\varepsilon)$ relation and considering the strain correction due to its non-uniformity along the sample

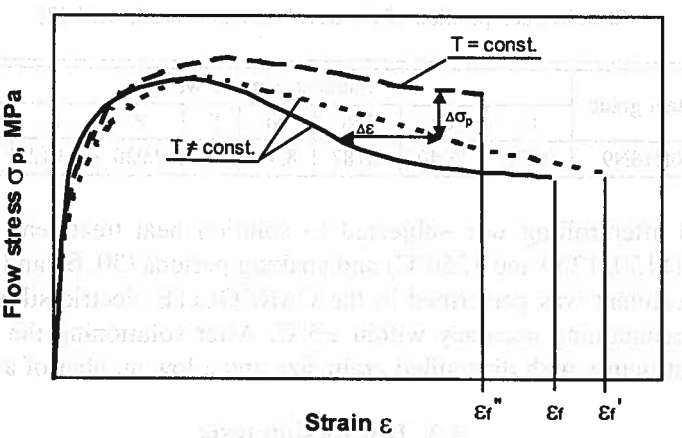

Fig. 3. The flow stress (dashed line) and strain to fracture (dotted line) corrections due to the strain localization and the temperature increase during torsion [11]: $\Delta\sigma_p$ — the increase of flow stress due to the increase of a sample temperature during torsion, $\Delta\varepsilon$ — the increase of strain due to the non-uniformity of strain along the sample gauge length

gauge length. A correction process of $\sigma_p = f(\varepsilon)$ relation for T = const and $\dot{\varepsilon}$ = const, considering the non-uniformity of strain and the temperature increase, is shown in Fig. 3.

2.4. Determination of a sample area for microstructure testing

A natural feature of the torsion test is the non-uniformity of strain over the sample cross-section. For proper analysis of the microstructure changes corresponding to the average strain over the sample cross-section $\overline{\varepsilon}$, determination of the equivalent radius $\overline{R}$ is required. If the assumption is made that the strain distribution along the sample radius R is linear, the equivalent radius is equal to $2/3R$. Strain in this area is equal to two-thirds of the strain calculated for the outer radius R.

3. Determination of technological plasticity characteristics for austenitic steel 0H18N9

A procedure for determination of plasticity characteristics in hot torsion test was elaborated and presented for austenitic steel grade 0H18N9 [7].

3.1. Material for test

The test material includes hot rolled rods of austenitic steel grade 0H18N9 with 19 mm dia. and chemical composition as presented in Table 1.

TABLE 1

Chemical composition of the tested austenitic steel, wt.% [7]

Steel grade	Element content, wt.%							
	C	Cr	Mn	Ni	Si	P	S	B
0H18N9	0.028	18.40	0.187	8.90	—	0.036	0.012	—

The steel after rolling was subjected to solution heat treatment. Three various temperatures (1150, 1200 and 1250°C) and soaking periods (30, 60 and 120 min) were used. Heat treatment was performed in the CARBOLITE electric silite furnace, with temperature maintaining accuracy within ±5°C. After solutioning the steel exhibited an austenitic structure with diversified grain size and a low number of annealing twins.

3.2. Hot torsion tests

Torsion tests were conducted on standard samples, having the shape and the size as given in Fig. 2a. To determine the non-uniformity of strain, a longitudinal scratch of 0.2 mm in depth was marked on the gauge surface of samples. Prior to deformation, samples were heated and soaked in temperature of 1200°C for 5 minutes. Then

they were cooled down to a nominal temperature of the torsion test and held in this temperature for 1 minute. Samples were subjected to torsion to fracture at a predefined constant twist rate (Fig. 4). Tests were carried out in the temperature range of 900 ÷ 1200°C and the twist rate range of 10 ÷ 1600 rpm. For making the analysis of structure evolution and the non-uniformity of strain possible, the rapid water-cooling system was used. After deformation, a measurement of the marked line inclination angle was conducted by means of the MWDC toolroom microscope equipped with the attachment for angle measurements.

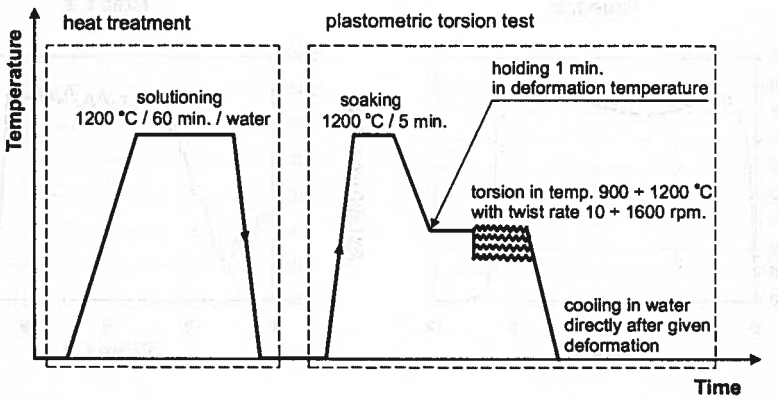

Fig. 4. Schedule of the performed experiment [7]

3.3. Elaboration of plastometric test results

3.3.1. Processing of measurement data

Determination of flow curves in the hot torsion test is based on the measurement data, i.e. torque M [Nm], axial force F [N], temperature T [°C], number of twists N [rot] and time t [s], registered in time intervals Δt by the plastometer data acquisition system and saved as text files. The data stored in text files can be easily imported by the Excel worksheet and presented in a form of charts. Some courses of recorded quantities as a function of time are shown in Fig. 5 as examples.

Processing of measurement data, involving filtration, trimming, decimation and smoothing, was made in the Matlab software. Spline smoothing was performed with the help of the Spline Tool graphical user interface.

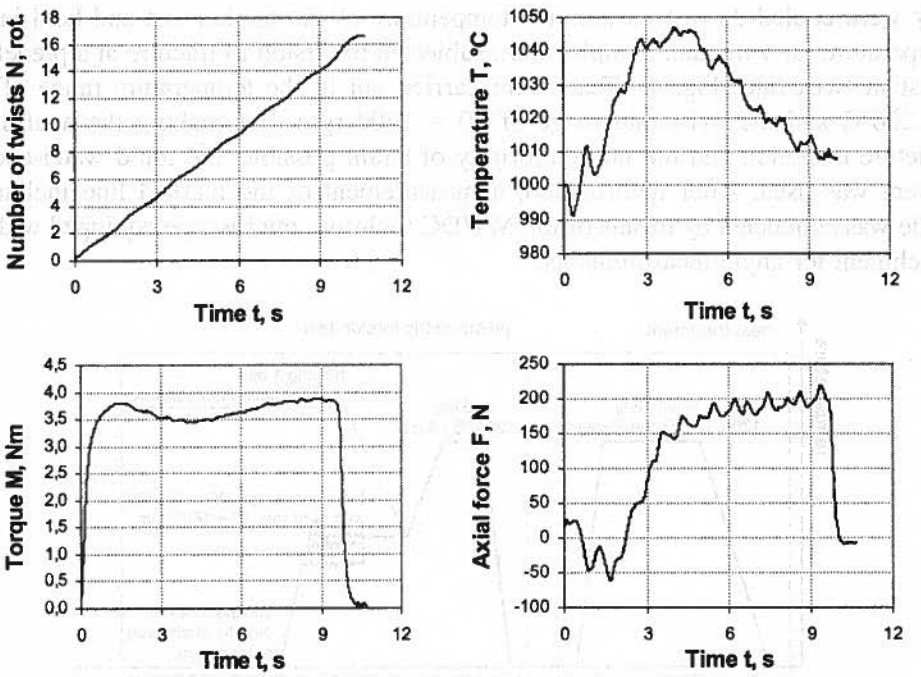

Fig. 5. Recorded values of torque, number of twists, temperature and axial force during the torsion test conducted on the 0H18N9 steel sample at temperature of 1000°C with a twist rate of 100 rpm [7]

3.3.2. Correction of torque

The acceleration of twist rate from zero to a nominal value takes place in the hot torsion test. Also the sample's temperature increases during torsion. These two phenomena causes the necessity of performing the recorded torque correction. The relation of twist rate on time is shown in Fig. 6. The time required to achieve the nominal twist rate is 0.4 ÷ 0.5 s. Correction of torque due to the twist rate discrepancy was made using the formula:

$$M' = \left(\frac{\dot{N}_z}{\dot{N}}\right)^m \cdot M, \tag{1}$$

where:

- M — recorded torque value, Nm,
- M' — torque value corrected due to the twist rate discrepancy, Nm,
- $\dot{N}$ — recorded twist rate, rpm,
- $\dot{N}_z$ — preset nominal twist rate, rpm,
- m — strain-rate sensitivity index.

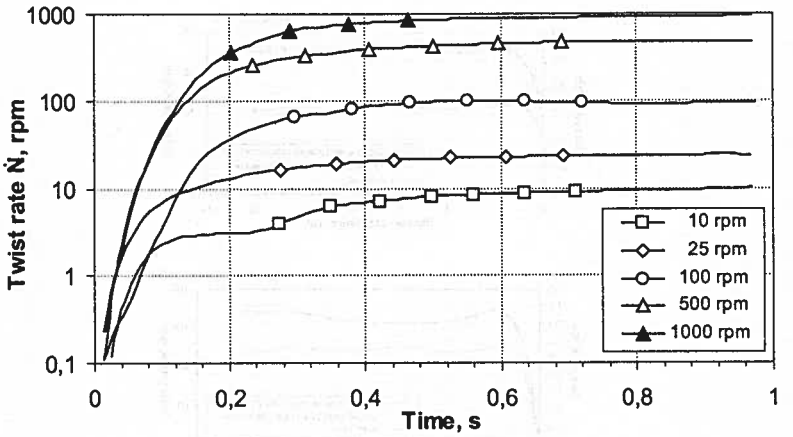

Fig. 6. Twist rate as a function of time [7]

The material sensitivity index m, required in calculations of the twist rate, is defined by approximation of $M = M(N, \dot{N}, T)$ values with the relation:

$$M = A \cdot N^B \cdot \exp(C \cdot N) \cdot \dot{N}^{D+\frac{E}{T}} \cdot \exp(\frac{F}{T}), \tag{2}$$

where

$$D + \frac{E}{T} = m. \tag{3}$$

The constants appearing in above equation were calculated using the least square method: $A = 0.011223$; $B = 0.111474$; $C = -0.0264$; $D = 0.31321$; $E = -148.051$; $F = 5002.817$.

Values of the m index for 0H18N9 steel were defined in nominal temperatures of torsion tests. They are given in Table 2.

TABLE 2

Strain rate sensitivity index (m) for 0H18N9 steel in various temperatures [7]

T,°C	900	1000	1100	1200
m	0.149	0.165	0.179	0.190

Recordings of twist rate and values of torque prior to and after correction as a function of the number of twists are shown in Fig. 7. For high twist rates of about 1000 rpm, the nominal speed is achieved after dozen twists of the sample (beyond a peak torque value) and leads to essential diversification of torque values prior to and after correction. For twist rates $\dot{N} = 10$ rpm and $\dot{N} = 100$ rpm diversification of torque prior to and after correction is insignificant.

Dependence of temperature and torque on the number of twists, obtained during torsion at nominal temperature of 1000°C for various twist rates is shown in Fig. 8.

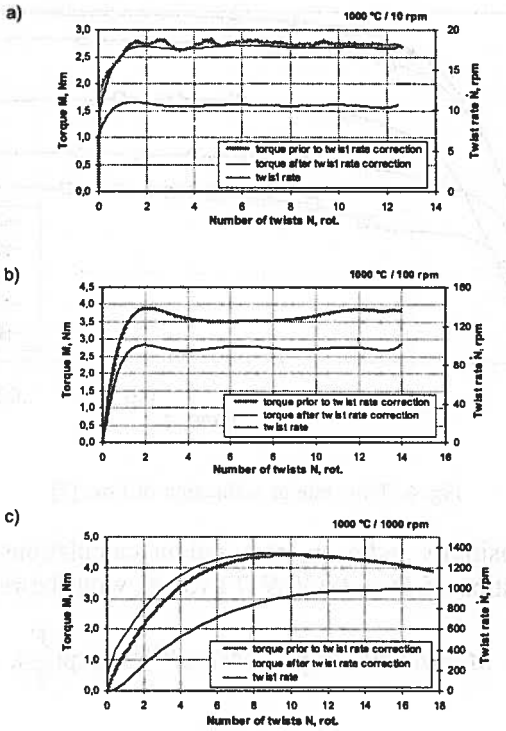

Fig. 7. Dependence of torque (prior to and after correction), and twist rate on the number of twists: a) T = 1000°C, $\dot{N}$ = 10 rpm, b) T = 1000°C, $\dot{N}$ = 100 rpm, c) T = 1000°C, $\dot{N}$ = 1000 rpm [7]

For the lowest twist rate ($\dot{N}$ = 10 rpm) fluctuations of temperature around the nominal value were observed, resulting from the interference of temperature control system. Fluctuations of temperature correspond to relevant fluctuations of the torque run. For the intermediate twist rate ($\dot{N}$ = 100 rpm), the temperature rise due to conversion of deformation work into heat occurs. After that, temperature falls to the nominal value. This results from reaction of the control system which is activated by a required temperature and a time increase. The temperature falling results in the torque value increase. For the highest twist rate ($\dot{N}$ = 1000 rpm), where the time of torsion to fracture is about 1 s, the control system would not have time to react to the temperature change. In this range of twist rates, a constant increase of temperature during torsion is observed.

Correction of torque considering the increase of temperature ΔT during torsion was calculated by the superposition method. Thus:

$$M'' = M' + \Delta M'', \tag{4}$$

where:

M' — torque value corrected due to the temperature discrepancy,

$\Delta M''$ — increment of torque due to the temperature discrepancy, calculated as:

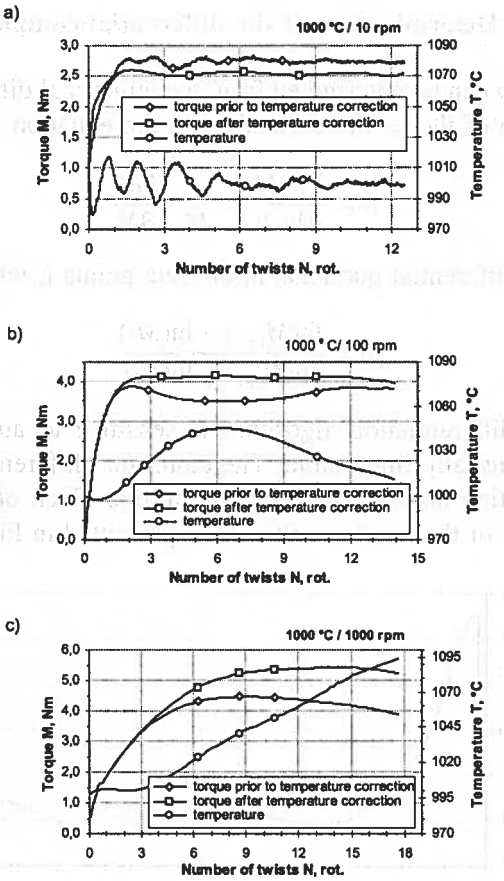

Fig. 8. Recorded values of temperature as well as recorded and corrected torque values as a function of the number of twists: a) T = 1000°C, $\dot{N}$ = 10 rpm, b) T = 1000°C, $\dot{N}$ = 100 rpm, c) T = 1000°C, $\dot{N}$ = 1000 rpm [7]

$$\Delta M'' = M(N, \dot{N}, T) - M(N, \dot{N}, T + \Delta T). \tag{5}$$

When using the relation (2) one can write that:

$$\begin{aligned} M'' = A \cdot N^B \cdot \exp(C \cdot N) \cdot \dot{N}^{D+\frac{E}{T}} \cdot \exp(\tfrac{F}{T}) - \\ -A \cdot N^B \cdot \exp(C \cdot N) \cdot \dot{N}^{D+\frac{E}{T+\Delta T}} \cdot \exp(\tfrac{F}{T+\Delta T}). \end{aligned} \tag{6}$$

Comparison of the torque curves prior to and after correction due to the temperature discrepancy is shown in Fig. 8.

3.3.3. Determination of the differential component *p*

The component p can be determined from the numerical differentiation algorithm, based on replacement of the partial derivatives in the equation:

$$p = \frac{\partial \ln M}{\partial \ln N} = \frac{N}{M} \cdot \frac{\partial M}{\partial N} \tag{7}$$

with the equivalent differential quotients in discrete points i, where $i = 2, 3, \ldots n$:

$$p_i = \frac{\ln(M_{i+1}) - \ln(M_i)}{\ln(N_{i+1}) - \ln(N_i)}. \tag{8}$$

The numerical differentiation algorithm is sensitive to any disturbances, so its direct application is usually impossible. Therefore, the differential component p was calculated after filtration and smoothing of the torque. Such obtained relation of the p-value as a function of the number of twists is presented in Fig. 9.

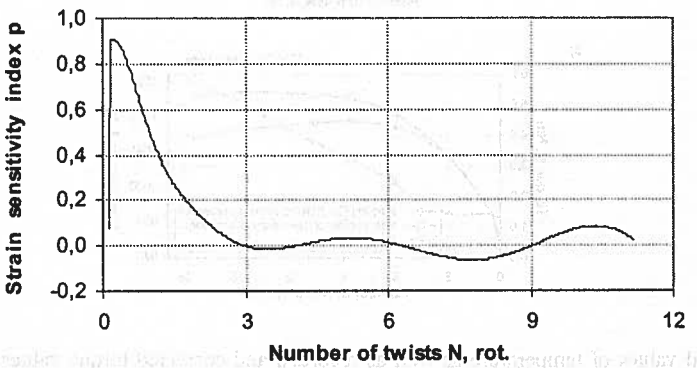

Fig. 9. Strain sensitivity index p as a function of the number of twists, calculated after smoothing the torque with a spline, T = 1000°C, $\dot{N}$ = 100 rpm [7]

3.3.4. Determination of the stress-strain curves

The flow stress, strain and strain rate were calculated using the classic formulas of torsion theory:

- flow stress,

$$\sigma_p = \sqrt{\left(\frac{\sqrt{3} \cdot M}{2 \cdot \pi \cdot R^3}\right)^2 \cdot (3 + p + m)^2 + \left(\frac{F}{\pi \cdot R^2}\right)^2} \tag{9}$$

- strain,

$$\varepsilon = \frac{2}{\sqrt{3}} \cdot \frac{\pi \cdot R \cdot N}{L} \tag{10}$$

- strain rate,

$$\dot{\varepsilon} = \frac{2}{\sqrt{3}} \cdot \frac{\pi \cdot R \cdot \dot{N}}{L}. \tag{11}$$

Correction of strain due to the non-uniformity of strain over the sample gauge length was performed according to formula:

$$\delta = \frac{\varepsilon_{\max}}{\varepsilon_m}, \tag{12}$$

where:

δ — the strain non-uniformity index,

ε_{max} — local strain corresponding to the maximum torsion angle α_{max} over the sample gauge length,

ε_m — average strain along the gauge length of a sample, calculated from the number of twists N, the diameter D and the gauge length L:

$$\varepsilon_m = \frac{\pi D \cdot N}{\sqrt{3}L} \tag{13}$$

The strain non-uniformity index δ can be defined from the measurement of the inclination angle of a scratch [11]. Dependence of δ index on temperature and twist rate is shown in Fig. 10. It was obtained by approximation of the $\delta = \delta(T, \dot{N})$ values with the relation:

$$\delta = A \cdot \dot{N}^B \cdot \exp(\frac{C}{T}). \tag{14}$$

The constants A, B, C in the equation (14) were calculated with the least square method: $A = 0.556973$; $B = 0.032046$; $C = 618.6959$.

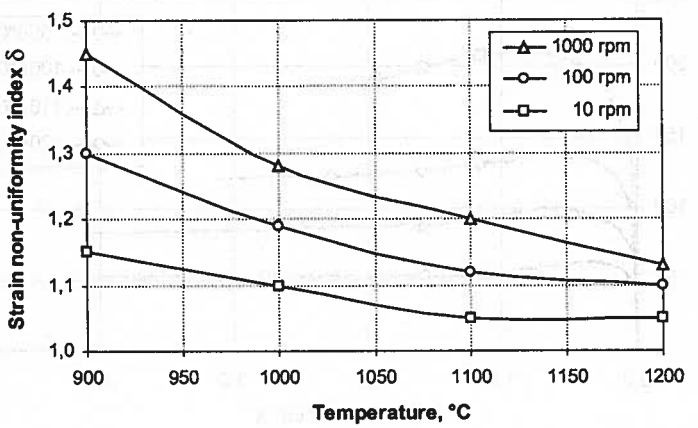

Fig. 10. Dependence of the strain non-uniformity index δ on temperature and twist rate [7]

Comparison of stress-strain curves prior to and after correction due to the non--uniformity of strain over the gauge length of twisted sample is shown in Fig. 11.

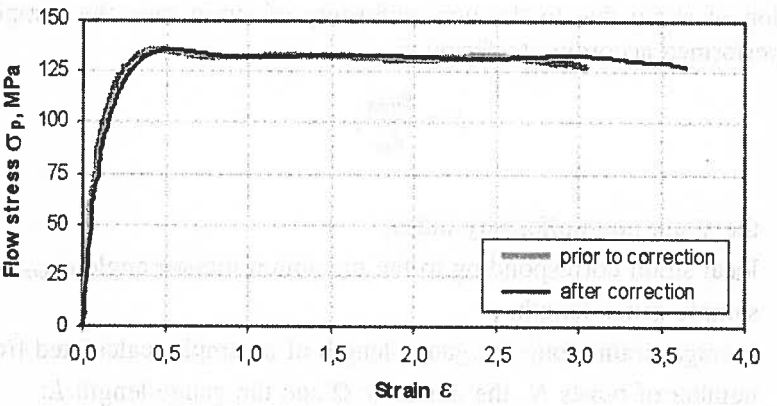

Fig. 11. Stress-strain curves before and after correction due to the non-uniformity of strain along the sample gauge length. T = 1000°C, $\dot{N}$ = 100 rpm [7]

3.3.5. Technological plasticity characteristics

A general evaluation of plasticity can be made basing on relations: $\sigma_p = \sigma_p(\varepsilon, \dot{\varepsilon}, T)$ and $\varepsilon_f = \varepsilon_f(\dot{\varepsilon}, T)$. They can be determined from the defined stress-strain curves for various temperatures and strain rates. The stress-strain curves for 0H18N9 steel at various deformation temperatures and for strain rate of 0.7 s^{-1} are presented in Fig. 12.

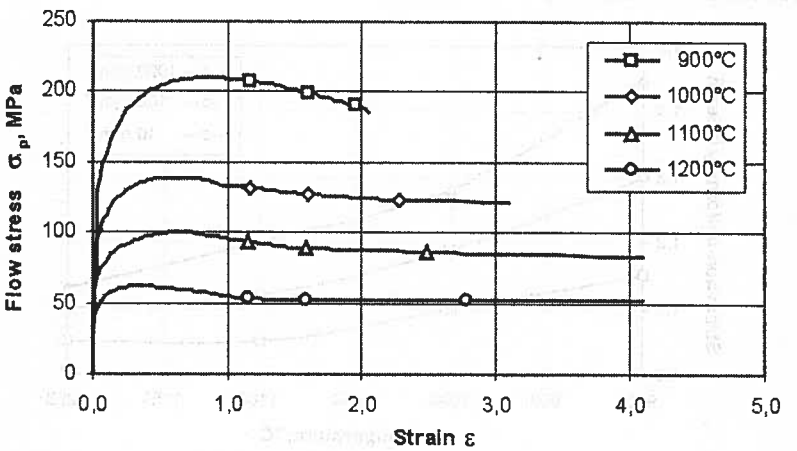

Fig. 12. Stress-strain curves at various deformation temperatures and for strain rate 0.7 s^{-1} [7]

The technological plasticity characteristics in the form of dependencies of peak stress σ_{pp}, peak strain ε_p and strain to fracture ε_f on temperature and strain rate are shown in Fig. 13.

a)

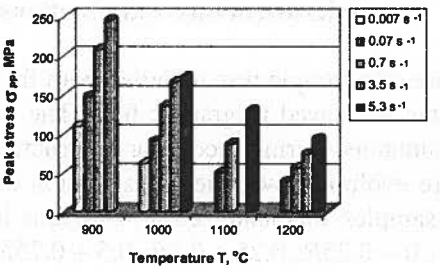

b)

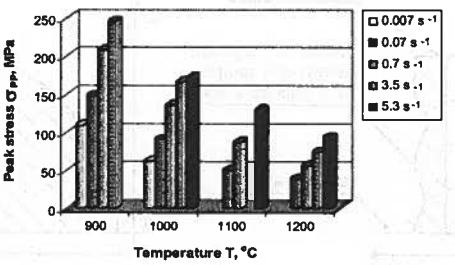

c)

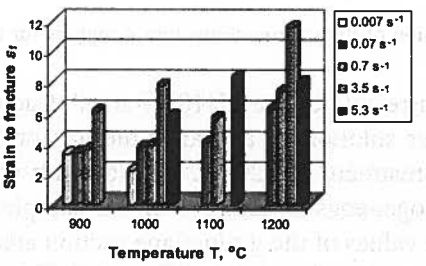

Fig. 13. Dependence of peak stress δ_{pp}, peak strain ε_p and strain to fracture ε_f on temperature and strain rate [7]

The Hensel-Spittel relation was adopted to describe the flow stress function in the form [12]:

$$\sigma_p = A \cdot \varepsilon^B \cdot \exp(C \cdot \varepsilon) \cdot \dot{\varepsilon}^{D+\frac{E}{T}} \cdot \exp(\frac{F}{T}). \tag{15}$$

The calculated constants in the equation (15) are as follows: A = 2.551077; B = 0.103816; C = −0.08356; D = 0.412724; E = −257.048; F = 4045.555.

The relationship (15) is valid in the strain range $0 < \varepsilon < \varepsilon_s$. The ε_s value corresponds to the beginning of the steady state. The value of steady-state stress σ_{ps} is usually equal to $0.8 \div 0.9\ \sigma_{pp}$.

3.4. Determination of a representative area for microstructure examinations

The microstructure of a sample was recorded with the help of a camera connected to a PC class computer and saved in graphic files. The orientation of metallographic microsections was maintained during recording of structures, as shown in Fig. 14. For estimation of structure evolution over the cross-section of a plastometric sample, the structure of selected samples was analyzed in 4 regions located at different distances from the sample axis: $0 \div 0.25R$; $0.25 \div 0.5R$; $0.5 \div 0.75R$; $0.75 \div 1.0R$.

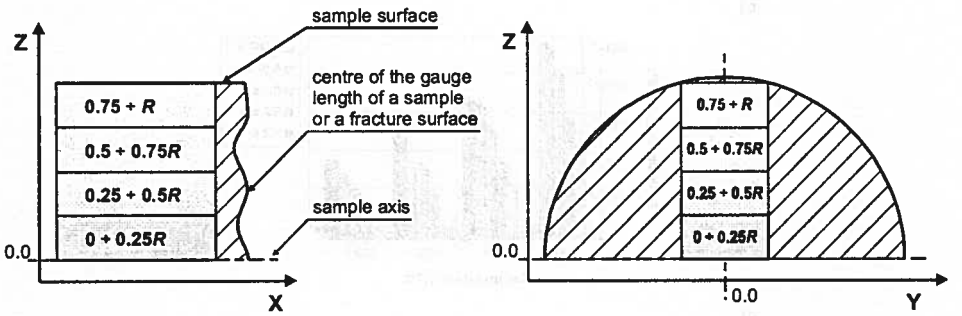

Fig. 14. Division of the microsections into 4 regions for the light microscopy [7]

The examination results of the 0H18N9 steel structure over the longitudinal sections of samples after solutioning and after the torsion test are presented in Table 3. After solution heat treatment at 1200°C with 60 min of soaking time, the 0H18N9T steel exhibits a homogeneous structure over the sample longitudinal section, what is confirmed by similar values of the grain plane section area $\overline{A}_0$ and the grain size heterogeneity index ($\overline{A}_0$) in regions located at different distances from the sample axis (Table 3). After deformation of 0H18N9 steel at temperature of 900°C, the heterogeneity of structure at the sample cross section is observed. This is manifested by a significant growth of the grain plane section average area $\overline{A}_0$ as well as by decreasing of the grain size heterogeneity index $\nu(\overline{A}_0)$ from the surface to the sample centre. The steel, after deformation at temperature of 1000 and of 1100°C causing dynamic recrystallization in the whole volume of a sample, shows small diversification of structure among particular regions over the longitudinal section of plastometric sample.

The results obtained confirm a necessity of performing the microstructure analysis in a strictly defined and reproducible region corresponding to the equivalent radius ($\overline{R} \cong 2/3R$) which is used in relationships for calculation of the average strain over the sample cross-section $\dot{\varepsilon}$.

TABLE 3

Variation of the average area $\overline{A}_0$ and heterogeneity $v(\overline{A}_0)$ of grain size over the sample longitudinal section [7]

Deformation parameters	Distance from a sample surface	0H18N9 steel	
		$\overline{A}_0$, μm^2	$v(\overline{A}_0)$, %
Initial state (before deformation) Solutioning – 1200°C	$0.75 \div 1.0R$	5904	105
	$0.5 \div 0.75R$	6053	120
	$0.25 \div 0.5R$	5714	111
	$0 \div 0.25R$	6200	131
900°C $0.7\ s^{-1}$	$0.75 \div 1.0R$	2300	162
	$0.5 \div 0.75R$	2881	146
	$0.25 \div 0.5R$	3200	121
	$0 \div 0.25R$	3715	118
1000°C $0.7\ s^{-1}$	$0.75 \div 1.0R$	161	134
	$0.5 \div 0.75R$	152	149
	$0.25 \div 0.5R$	143	142
	$0 \div 0.25R$	109	140
1100°C $0.7\ s^{-1}$	$0.75 \div 1.0R$	431	125
	$0.5 \div 0.75R$	424	124
	$0.25 \div 0.5R$	456	132
	$0 \div 0.25R$	413	118

4. Summary

Correctness in determination of technological plasticity characteristics depends on the adopted research method, modernity of the test stand available as well as on the applied methodology for testing and for processing of obtained test results. The lack of general standards in this field causes discrepancies among results obtained in various research centres. Among the factors having influence on such discrepancies one can mention: the thermal effect, gradient of temperature over the sample cross-section, non-uniformity of strain, the sample preparation method and the formulas used in calculations of the relationship between the flow stress and strain from recorded experimental data. The described procedure, which is used for determination of relationship between the flow stress and strain on the basis of performed hot torsion tests, considers preparation of samples for plastometric tests, heating of samples, elaboration of torsion test results and the method of sample preparation for microstructure examinations.

REFERENCES

[1] F. Grosman, E. Hadasik, A. Sobański, Rozwój metodyki i zastosowań plastometrycznej próby skręcania. Inżynieria Materiałowa **1**, 20-25 (1985).

[2] F. Grosman, E. Hadasik, M. Hetmańczyk, N. Smyczek, Prognozowanie odkształcalności wlewków ze stali 1H18N9T w oparciu o wyniki badań plastometrycznych. Nowe poznatky v tvareni kovu, Frydland nad Ostravici, 50-58, 12- 14.09.1995.

[3] H. Pircher, R. Kawalla, H.P. Schmitz, F. Grosman, E. Hadasik, D. Ćwiklak, Badania plastyczności stali niskowęglowych przeznaczonych do walcowania w zakresie ferrytu. Plastyczność materiałów, Plast'96, 161-167, Ustroń, 25–28.09.1996.

[4] M. Siwek, E. Hadasik, G. Sołtysik, Zastosowanie plastometru skrętnego w Hucie Baildon. Plastyczność Materiałów, Plast'94, 137-142, Wisła, 29–30.9.1994.

[5] A. Sobański, E. Hadasik, Die Aussagefühigkeit von Versuchen mit dem Torsionplastometer. Stahl und Eisen 16, 66-76 (1980).

[6] A. Sobański, E. Hadasik, A. Piątek, Niektóre doświadczenia nad wykorzystaniem plastometru skrętnego w badaniach materiałów. Inżynieria Materiałowa, 214-217, No. 6(7) 1981.

[7] E. Hadasik, Metodyka wyznaczania charakterystyk plastyczności w próbie skręcania na gorąco. Politechnika Śląska, Hutnictwo No 63, Gliwice 2002.

[8] Z. Gronostajski, E. Hadasik, I. Schindler, Analiza próby skręcania na gorąco metodą elementów skończonych. Zastosowanie komputerów w zakładach przetwórstwa metali, 103-110, KomPlasTech 2002, Szczawnica 13 – 16.01.2002.

[9] E. Hadasik, A. Sobański, Wpływ wymiarów próbki na wyniki próby skręcania. Zastosowanie badań plastometrycznych w przeróbce plastycznej metali, 54-60, Częstochowa, October 1981.

[10] K. Kurek, E. Hadasik, Optymalizacja wzbudnika nagrzewnicy indukcyjnej plastometru skrętnego metodą symulacji komputerowej 43-47, Forming'97, Rožnov pod Radhostem, 2-4.09.1997.

[11] F. Grosman, E. Hadasik, Problemy zastosowania charakterystyk technologicznej plastyczności w komputerowych programach analizy i projektowania procesów przeróbki plastycznej. Archiwum Hutnictwa **3**, 263-276 (1994).

[12] A. Hensel, T. Spittel, Kraft- und Arbeitsbedarf bildsomer Formgeburgs-Verfahren. VEB Deutscher Verlag fur Grundstoffindustrie, Lipsk 1979.

Received: 4 October 2004.

This work was supported by the Polish Committee for Scientific Research, under grant No 4 T08A 02922.